How to cite: *Angew. Chem. Int. Ed.* **2022,** *61,* e202117499
International Edition: doi.org/10.1002/anie.202117499
German Edition: doi.org/10.1002/ange.202117499

Organometallic Chemistry

A Highly Fluorescent Dinuclear Aluminium Complex with Near-Unity Quantum Yield**

*Flavio L. Portwich, Yves Carstensen, Anindita Dasgupta, Stephan Kupfer, Ralf Wyrwa, Helmar Görls, Christian Eggeling, Benjamin Dietzek, Stefanie Gräfe, Maria Wächtler, and Robert Kretschmer**

Dedicated to Professor Heinrich Lang on the occasion of his 65th birthday

[*] F. L. Portwich, Dr. H. Görls, Prof. Dr. R. Kretschmer
Institute of Inorganic and Analytical Chemistry (IAAC)
Friedrich Schiller University Jena
Humboldtstraße 8, 07743 Jena (Germany)
E-mail: robert.kretschmer@uni-jena.de

Y. Carstensen, Dr. S. Kupfer, Prof. Dr. B. Dietzek, Prof. Dr. S. Gräfe, Dr. M. Wächtler
Institute of Physical Chemistry
Friedrich Schiller University Jena
Helmholtzweg 4, 07743 Jena (Germany)

A. Dasgupta, Prof. Dr. C. Eggeling, Prof. Dr. B. Dietzek, Dr. M. Wächtler
Leibniz Institute of Photonic Technology
Albert-Einstein-Straße 9, 07745 Jena (Germany)

A. Dasgupta, Prof. Dr. C. Eggeling
Institute of Applied Optics and Biophysics
Friedrich Schiller University Jena
Helmholtzweg 4, 07743 Jena (Germany)

Dr. R. Wyrwa
INNOVENT e. V. Technologieentwicklung Jena
Prüssingstraße 27 B, 07745 Jena (Germany)

Prof. Dr. C. Eggeling, Prof. Dr. B. Dietzek, Prof. Dr. S. Gräfe, Dr. M. Wächtler
Abbe Center of Photonics
Friedrich Schiller University Jena
Albert-Einstein-Straße 6, 07745 Jena (Germany)

Prof. Dr. C. Eggeling
MRC Human Immunology Unit, Weatherall Institute of Molecular Medicine
University of Oxford
Oxford OX39DS (UK)

Prof. Dr. C. Eggeling, Prof. Dr. B. Dietzek, Prof. Dr. R. Kretschmer
Jena Center for Soft Matter (JCSM)
Friedrich Schiller University Jena
Philosophenweg 7, 07743 Jena (Germany)

Prof. Dr. S. Gräfe
Fraunhofer Institute for Applied Optics and Precision Engineering (Fraunhofer IOF)
Albert-Einstein-Str. 7, 07745 Jena (Germany)

[**] A previous version of this manuscript has been deposited on a preprint server (https://doi.org/10.26434/chemrxiv-2021-hd1ck).

Abstract: The high natural abundance of aluminium makes the respective fluorophores attractive for various optical applications, but photoluminescence quantum yields above 0.7 have yet not been reported for solutions of aluminium complexes. In this contribution, a dinuclear aluminium(III) complex featuring enhanced photoluminescence properties is described. Its facile one-pot synthesis originates from a readily available precursor and trimethyl aluminium. In solution, the complex exhibits an unprecedented photoluminescence quantum yield near unity ($\Phi_{absolute}$ 1.0 ± 0.1) and an excited-state lifetime of 2.3 ns. In the solid state, J-aggregation and aggregation-caused quenching are noted, but still quantum yields of 0.6 are observed. Embedding the complex in electrospun non-woven fabrics yields a highly fluorescent fleece possessing a quantum yield of 0.9 ± 0.04.

Fluorescent compounds based on main-group elements are of fundamental interest as they combine favorable electrochemical, photophysical, and spectroscopic properties with the high natural abundance of many of the s- and p-block elements. Therefore, related fluorophores have found numerous applications, for example, in bioimaging,[1] chemosensing[1b,2] or as materials for organic light-emitting diodes (OLEDs).[3] However, although many of the main-group elements are more abundant than 2nd and 3rd row transition metals, the supply of certain elements such as boron, germanium, and bismuth is at (future) risk.[4] In light of the broad applications of boron-containing dyes like BODIPY and derivatives,[1a,5] developing fluorophores based on its non-endangered relative aluminium is a highly desirable task. In the late 1980s, tris(8-hydroxyquinolinato)aluminium(III) (Alq3) was used to develop the first thin-film light-emitting diode,[6] wherefore the development of aluminium complexes with improved emission efficiencies received considerable interest. While at the beginning, most of the studies were focused on modifications of the 8-hydroxyquinoline ligand,[3e,7] the last decade has witnessed the development of new aluminium-containing fluorophores with improved photophysical properties.[8] But although the photoluminescence quantum yields in solution have been significantly improved from 0.2 in the case of Alq3[9] and 0.4 for Al–salen complexes[8c] up to

0.7 for an aluminium N_2O_2–dipyrrin complex,[8b] they still cannot compete with dyes based on their lighter or heavier Group 13 relatives such as BODIPY[10] or GADIPY,[11] possessing fluorescence quantum yields (in toluene) of 0.8 and 0.9, respectively (Figure 1). In this contribution, we present a readily available dinuclear aluminium(III) complex (**1**) possessing an unprecedented photoluminescence quantum yield up to 1.0 in solution, which adds information to the yet under-explored photochemistry of dinuclear complexes.[12]

Complex **1** is conveniently prepared in good yield from the β-oxo-δ-diimine **(BODDI)H$_2$**[13] and trimethylaluminium

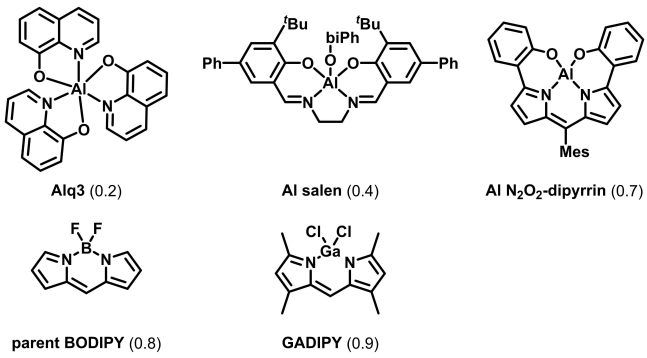

Figure 1. Selected structures of Group 13 dyes along with quantum yields (given in brackets) reported for solutions; biPh: 4-biphenyl, Mes: mesitylene.

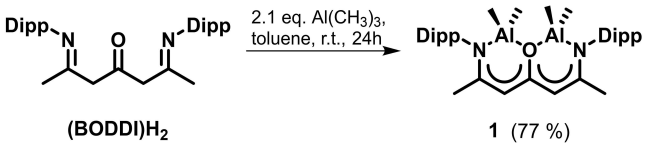

Scheme 1. Complex **1** is readily prepared from the protio-ligand **(BODDI)H$_2$**.

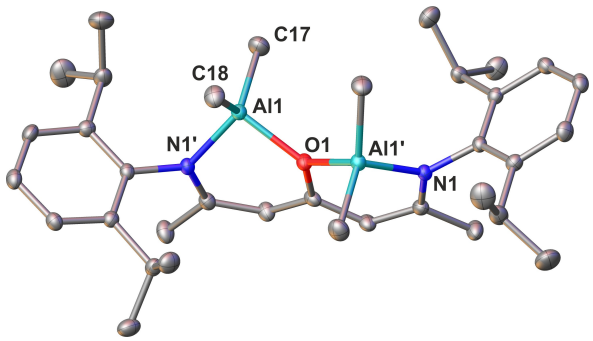

Figure 2. Molecular solid-state structure of **1** with hydrogen atoms omitted for clarity; symmetry operation for atoms marked with ′ : $1-x, +y, 3/2-z$. Selected bond lengths [Å] and angles [°] with calculated values [B3LYP10/def2svp/SMD(toluene)] in square brackets: Al1–N1′ 1.9004(12) [1.927], Al1–O1 1.8938(8) [1.913], Al1–C17 1.9562(15) [1.968], Al1–C18 1.9575(16) [1.963], N1′–Al1–O1 95.28(5) [92.5], C17–Al1–C18 118.58(7) [122.3]. The computed structure is shown in Figure S4.

(Scheme 1). Its molecular structure in the solid state (Figure 2),[14] resembles structural features of previously reported β-oxo-δ-diimine complexes of lutetium and zinc:[13a,15] the two tetrahedral coordinated aluminium centers are chelated in a κ^1-N:μ^2-O:κ^1-N fashion and reside on opposite sites and 0.74 Å above and below the almost planar BODDI backbone. The Al–C, Al–N, and Al–O bond lengths are in good agreement with related dinuclear complexes based on N,O-chelating ligands.[16] The packing of **1** in the crystal structure (Figures S1–S3) is strongly affected by the steric demands of the 2,6-diisopropylphenyl (Dipp) groups, which is why neither dispersive intermolecular interactions between the π-systems nor any well-defined interaction with the backbone of the BODDI ligand are observed. The molecules are packed into two-dimensional sheets and the molecules of two adjacent layers are facing each other. A simple set of ^{1}H NMR resonances of the Dipp groups (two methyl doublets and one methine septet), of the BODDI-backbone (one methyl and one methine singlet), and the $Al(CH_3)_2$ groups (one singlet) indicates a C_{2v}-symmetric or averaged structure in solution (C_6D_6). A cyclic voltammetry experiment of **1** reveals one reversible reduction event occurring at −2.21 V and one irreversible oxidation at 0.38 V with respect to Fc/Fc^+ in acetonitrile (Figure S5). Similar to other alkylaluminium complexes, **1** is sensitive towards hydrolysis forming back the (non-fluorescent) protio-ligand. However, when using dry solvents, **1** can be processed under aerobic conditions for example in electrospinning (see below). **(BODDI)H$_2$** is also formed upon alcoholysis, which has been reported before for mono- and dinuclear alkylaluminium complexes.[17] **1** is thermally stable in the solid state, i.e., it melts without decomposition at 220.5 °C, and solutions in $CDCl_3$ or THF-d_8 show no indication of decomposition when heated under inert conditions for three days to 60 °C (Figure S21—26).

1 features a pronounced fluorescence both in solution and in the solid state, Figure 3, which, however, is significantly affected by the sample type. Hence, the photophysical properties of **1** in solution, as powder and as crystalline material were investigated by steady-state absorption and fluorescence spectroscopy (Table 1). The absorption spectrum of a solution of **1** in toluene reveals one narrow peak at 455 nm. Quantum chemical investigations at the B3LYP10/def2SVP/SMD(toluene) level of theory allowed to assign this absorption feature to the excitation into the S_1

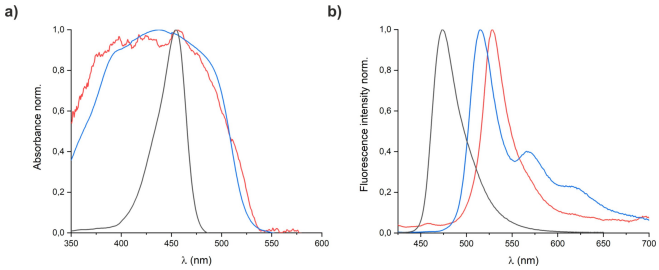

Figure 3. Normalized a) absorption and b) emission spectra of complex **1** as a single-crystal (red), powder sample (blue), and in toluene solution (1.40 μM, black).

Table 1: Selected experimental and computational photophysical properties of **1**; see Supporting Information for experimental details.

	λ_{max} [nm]	λ_{em} [nm]	$\Phi_{absolute}$	τ [ns]
1 (toluene)	455	471	1.0 ± 0.1	2.3
1 (TDDFT)	402	435	–	–
1 (powder)	438	515	0.5 ± 0.02	–
1 (crystal)	457	528	0.6 ± 0.07	1.8–2.5
1 (fleece)	327 and 387	490	0.9 ± 0.04	2.2–2.3

state of ππ* nature (at 402 nm) (Figure 4a). The sample gives rise to a blue emission that is centered at 471 nm, i.e., associated with a Stokes shift of 747 cm^{-1} and solutions of **1** in acetonitrile and dichloromethane give similar emission spectra with emission maxima at 471 and 472 nm, respectively (Figure S6). The absence of pronounced solvatochromism indicates that the polarity of the solvent does not appreciably perturb the ground or excited state. This finding is in agreement with the computational data on the emission of **1**. Structural relaxation of the S_1 state from the Franck–Condon point yields the equilibrium of the formerly excited ππ* state with merely slight structural rearrangement (see Table S5 for details). In consequence, an emission wavelength of 435 nm is predicted by quantum chemical calculations. Thus, the Stokes shift obtained at the time-dependent density functional theory (TDDFT) level is in good agreement with the experimental reference, i.e. 556 cm^{-1} versus 747 cm^{-1}, and reflects the marginal structural rearrangement as well as the locally excited nature of the ππ* transition and the absence of charge-transfer contributions (Figure 4b, ππ* equilibrium). In addition to this radiative relaxation pathway, a non-radiative relaxation channel is in principle available but is inhibited by a barrier—correlated to a stretch of the Al1–C17 bond—within the potential

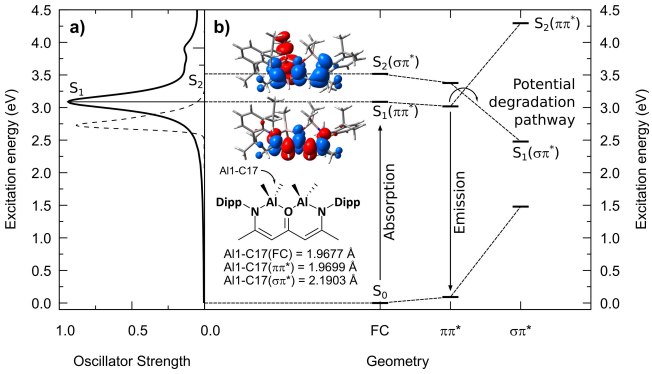

Figure 4. a) Experimental (in black, dashed) and simulated (in black, solid) UV/Vis absorption spectrum of 1 in toluene; prominent electronic transitions are indicated. b) Energy levels of the singlet ground state (S_0) as well as of the excited states S_1 (ππ*, strongly dipole-allowed) and S_2 (σπ*, dipole-forbidden) within their fully optimized equilibrium structures. Charge density differences (CDDs) indicate the electronic nature of S_1 (ππ*) and S_2 (σπ*). Emission occurs from the ππ* state. A radiation-less decay channel associated to photodegradation, i.e., cleavage of the Al1–C17 bond (see inset), might be accessible upon thermal activation and population of a σπ* state.

energy surface of the (adiabatic) S_1 state. Relaxation along this coordinate leads to a pronounced stabilization of the S_2 σπ* state and, in consequence, to an elongation of the Al1–C17 bond from 1.9677 Å within the Franck-Condon point (and 1.9699 Å within the ππ* equilibrium structure) to 2.1903 Å in the equilibrium structure of the σπ* state. This stretch of the Al–CH_3 bond results from the electronic configuration within the excited (σπ*) state, with the respective σ-orbital being only singly occupied—reducing its bond order to 0.5. Accordingly, the σπ*-S_0 gap is lowered to approximately 1 eV (Figure 4b, σπ* equilibrium structure) by the pronounced stabilization of the σπ* state and the destabilization of the electronic ground state upon elongation of the Al1–C17 bond. The population of this excited state relaxation pathway might impact the long-term photostability of **1** as it eventually leads to photodegradation by cleavage of the Al1–C17 bond as a result of the reduced bond order in the excited state.

In contrast to the behavior in solution, the powder and the crystalline samples give rise to broad absorption bands with maxima at 438 nm and 457 nm, respectively, and show a green emission although with differing emission spectra. The crystalline material features a single peak with an emission maximum at 528 nm (Stokes shift of 2942 cm^{-1}) while in case of the powder, a maximum at 515 nm (Stokes shift of 3414 cm^{-1}) is accompanied by two smaller peaks at 556 and 615 nm. Such pronounced Stokes shifts clearly point to the formation of aggregates in the solid, which lead, in consequence, to the emerging of low-lying intermolecular charge-transfer states.[18] This agrees well with the observed solid-state structure of **1**, which features characteristics of J-aggregates.[19] Aiming to obtain further insight, the quantum yield, as well as the fluorescence lifetime, have been investigated in toluene solution and in the solid state.

A value near unity ($\Phi_{absolute}$ 1.05 ± 0.1; $\Phi_{relative,perylene}$ 1.08 ± 0.09) was observed for the quantum yield of a toluene solution of **1** by absolute and relative measurements, which is, to the best of our knowledge, reported here for the first time.[20] The high quantum yield is well reflected by the strong dipole-allowed nature of both the $S_1 \leftarrow S_0$ as well as the $S_1 \rightarrow S_0$ transitions associated with the initial absorption process as well as to emission as obtained by TDDFT. When stored under aerobic conditions for two weeks, the toluene solution of **1** still possesses a quantum yield of about 0.5. Furthermore, based on a photochemical stability experiment (Figure S14), photodegradation via the σπ*-channel (see Figure 4b) seems to be unlikely. The excited state has an intrinsic lifetime (τ_0) of 2.3 ns (Figure S7) and a radiative decay rate k_r of 4.4×10^8 s^{-1}.

In the solid state, quantum yields of 0.5 for the powder and 0.6 for the crystalline sample have been obtained. In a control experiment, mixtures of **1** and barium sulfate in various ratios were thoroughly ground and investigated (see Supporting Information for details), and extrapolation to infinite dilution gave a quantum yield of 0.5. The reduced emission quantum yield in the solid samples can be related to aggregation-caused quenching (ACQ)[21] due to a reduced degree of intramolecular rotation particularly about the C–CH_3 bonds of the BODDI backbone. The crystals of **1**

feature a distribution of excited state lifetime in the range of 1.8 to 2.5 ns (Figure S8), which has been established by means of fluorescence-lifetime imaging (FLIM)[22] and is in good agreement with the lifetime in solution.

Electrospun luminescent nanofibers are of high value and have been used in a variety of photonic and optoelectronic applications.[23] Hence, **1** was embedded in elastic nonwoven polymer fabrics by electrospinning of a tetrahydrofuran solution of **1** and polystyrene (1.8 and 16.2 wt %). The resulting flexible highly-fluorescent yellow-green fleece is easy to handle and cut (Figure 5a). Fluorescence lifetime and scanning electron microscopy (SEM) images evidence the formation of beaded nanofibers with a smooth surface (Figure 5b,c). Please note that bead formation has been reported before and was attributed to various parameters.[24] As spinning of a control sample containing only polystyrene gave a colorless fabric showing significantly reduced bead formation (Figures S10a and S11), we assume that the addition of **1** lowers the surface tension of the solution, and, hence, the increased bead formation. The fibers feature two absorption maxima at 327 and 387 nm (Figure S13), and upon excitation at 410 nm the material possesses an intense blue fluorescence ($\lambda_{em}=490$ nm) with a quantum yield of 0.9 ± 0.04. When stored in air or in a desiccator, the quantum yield slowly decreases over time but after four weeks, still values of 0.7 and 0.8, respectively, are observed. Finally, the excited state lifetime was again obtained by FLIM experiments, and although slight deviations between strains and beads could be recognized, the mean value of 2.3 ns is reminiscent of those data obtained for the crystal or a toluene solution of **1**.

In summary, we have discovered the novel dinuclear main-group metal complex **1** that is readily available and possesses strong fluorescence. Toluene solutions of **1** exhibit a near-unity quantum yield ($\Phi_{absolute}$ 1.0 ± 0.1), which is unprecedented for aluminium(III) compounds, and caused by the strong dipole-allowed nature of both the absorption and the emission process. J-aggregation and aggregation-caused quenching give rise to a lower but still high photoluminescence quantum yield of 0.6. If the complex is embedded in electrospun non-woven fabrics, a highly fluorescent fleece with a quantum yield of 0.9 ± 0.04 is obtained. We are currently investigating routes towards other homo- and heterodinuclear complexes based on the β-oxo-δ-diimine ligand including those of B^{III}, Ga^{III}, and In^{III}, aiming to adopt and improve the photophysical properties relevant for different optical applications. Furthermore, experiments to modify the ligand system with respect to the backbone and the terminal substituents are under way as well.

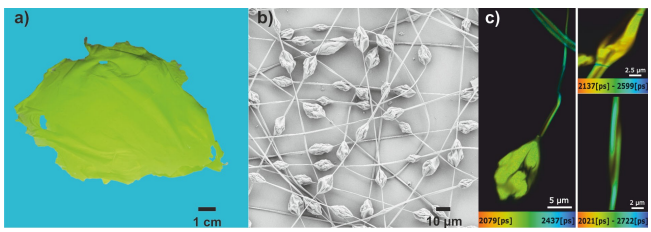

Figure 5. a) Photograph, b) SEM and c) FLIM micrographs of a non-woven polystyrene fabric containing **1**.

Acknowledgements

The project was financially supported by the Deutsche Forschungsgemeinschaft (DFG, KR4782/3-1 and 36454990-TRR234, CataLight, Z2, Germany's Excellence Strategy—EXC 2051—Project-ID 390713860, project number 316213987—SFB 1278 "PolyTarget", and INST 1757/25-1 FUGG), the Fonds der Chemischen Industrie and the Friedrich Schiller University Jena. We thank the Rechenzentrum of the Friedrich Schiller University Jena for the allocation of computer time, Fabian Seifert, and Raktim Baruah for helpful discussions, Florian C. Walter for assistance with the cyclic voltammetry experiments, Angelika Henning for EDX and SEM investigations, Cindy Altmann for carrying out the electrospinning and Dr. Mathias Micheel for STREAK camera measurements. Open Access funding enabled and organized by Projekt DEAL.

Conflict of Interest

The authors declare no conflict of interest.

Data Availability Statement

The data that support the findings of this study are available in the supplementary material of this article.

Keywords: Aluminium · Dinuclear Complexes · Fluorophores · Luminescence · Quantum Yield

[1] a) A. Loudet, K. Burgess, *Chem. Rev.* **2007**, *107*, 4891–4932; b) P. Kaur, K. Singh, *J. Mater. Chem. C* **2019**, *7*, 11361–11405; c) J. C. Berrones-Reyes, C. C. Vidyasagar, B. M. Muñoz Flores, V. M. Jiménez-Pérez, *J. Lumin.* **2018**, *195*, 290–313.

[2] a) N. Boens, V. Leen, W. Dehaen, *Chem. Soc. Rev.* **2012**, *41*, 1130–1172; b) T. Kawashima, T. Agou, J. Yoshino in *Comprehensive Inorganic Chemistry II, Second Edition* (Eds.: J. Reedijk, K. Poeppelmeier), Elsevier, Amsterdam, **2013**; c) D. Wu, A. C. Sedgwick, T. Gunnlaugsson, E. U. Akkaya, J. Yoon, T. D. James, *Chem. Soc. Rev.* **2017**, *46*, 7105–7123.

[3] a) S. Wang, *Coord. Chem. Rev.* **2001**, *215*, 79–98; b) X. Yang, G. Zhou, W.-Y. Wong, *Chem. Soc. Rev.* **2015**, *44*, 8484–8575; c) H. Xu, R. Chen, Q. Sun, W. Lai, Q. Su, W. Huang, X. Liu, *Chem. Soc. Rev.* **2014**, *43*, 3259–3302; d) Q. Wei, N. Fei, A. Islam, T. Lei, L. Hong, R. Peng, X. Fan, L. Chen, P. Gao, Z. Ge, *Adv. Opt. Mater.* **2018**, *6*, 1800512; e) C. Bizzarri, E. Spuling, D. M. Knoll, D. Volz, S. Bräse, *Coord. Chem. Rev.* **2018**, *373*, 49–82.

[4] N. R. Council, *The Role of the Chemical Sciences in Finding Alternatives to Critical Resources.* A Workshop Summary, The National Academies Press, Washington, DC, **2012**.

[5] a) L. J. Patalag, L. P. Ho, P. G. Jones, D. B. Werz, *J. Am. Chem. Soc.* **2017**, *139*, 15104–15113; b) Z. Liu, Z. Jiang, M.

Yan, X. Wang, *Front. Chem.* **2019**, *7*, 712; c) L. J. Patalag, J. Hoche, M. Holzapfel, A. Schmiedel, R. Mitric, C. Lambert, D. B. Werz, *J. Am. Chem. Soc.* **2021**, *143*, 7414–7425; d) P. Shrestha, K. C. Dissanayake, E. J. Gehrmann, C. S. Wijesooriya, A. Mukhopadhyay, E. A. Smith, A. H. Winter, *J. Am. Chem. Soc.* **2020**, *142*, 15505–15512; e) A. Atilgan, M. M. Cetin, J. Yu, Y. Beldjoudi, J. Liu, C. L. Stern, F. M. Cetin, T. Islamoglu, O. K. Farha, P. Deria, et al., *J. Am. Chem. Soc.* **2020**, *142*, 18554–18564; f) E. Y. Zhou, H. J. Knox, C. Liu, W. Zhao, J. Chan, *J. Am. Chem. Soc.* **2019**, *141*, 17601–17609.

[6] a) C. W. Tang, S. A. VanSlyke, *Appl. Phys. Lett.* **1987**, *51*, 913–915; b) D. Z. Garbuzov, V. Bulović, P. E. Burrows, S. R. Forrest, *Chem. Phys. Lett.* **1996**, *249*, 433–437.

[7] a) C. H. Chen, J. Shi, *Coord. Chem. Rev.* **1998**, *171*, 161–174; b) L. S. Sapochak, A. Padmaperuma, N. Washton, F. Endrino, G. T. Schmett, J. Marshall, D. Fogarty, P. E. Burrows, S. R. Forrest, *J. Am. Chem. Soc.* **2001**, *123*, 6300–6307; c) V. A. Montes, R. Pohl, J. Shinar, P. Anzenbacher, *Chem. Eur. J.* **2006**, *12*, 4523–4535; d) M. Albrecht, M. Fiege, O. Osetska, *Coord. Chem. Rev.* **2008**, *252*, 812–824; e) D. Singh, V. Nishal, S. Bhagwan, R. K. Saini, I. Singh, *Mater. Des.* **2018**, *156*, 215–228.

[8] a) P. G. Cozzi, L. S. Dolci, A. Garelli, M. Montalti, L. Prodi, N. Zaccheroni, *New J. Chem.* **2003**, *27*, 692–697; b) C. Ikeda, S. Ueda, T. Nabeshima, *Chem. Commun.* **2009**, 2544–2546; c) K. Y. Hwang, H. Kim, Y. S. Lee, M. H. Lee, Y. Do, *Chem. Eur. J.* **2009**, *15*, 6478–6487; d) M. Saikawa, M. Daicho, T. Nakamura, J. Uchida, M. Yamamura, T. Nabeshima, *Chem. Commun.* **2016**, *52*, 4014–4017; e) Y. Tong, B. Liu, Y. Wu, B. Yang, G. Wen, Y.-T. Yang, J. Chai, X. Hu, *Sens. Actuators B* **2017**, *252*, 794–802; f) S. W. Kwak, H. Jin, H. Shin, J. H. Lee, H. Hwang, J. Lee, M. Kim, Y. Chung, Y. Kim, K. M. Lee, M. P. Park, *Chem. Commun.* **2018**, *54*, 4712–4715; g) S. Bestgen, C. Schoo, B. L. Neumeier, T. J. Feuerstein, C. Zovko, R. Köppe, C. Feldmann, P. W. Roesky, *Angew. Chem. Int. Ed.* **2018**, *57*, 14265–14269; *Angew. Chem.* **2018**, *130*, 14461–14465; h) J. Li, P. Wu, W. Jiang, B. Li, B. Wang, H. Zhu, H. W. Roesky, *Angew. Chem. Int. Ed.* **2020**, *59*, 10027–10031; *Angew. Chem.* **2020**, *132*, 10113–10117; i) T. Ono, K. Ishihama, A. Taema, T. Harada, K. Furusho, M. Hasegawa, Y. Nojima, M. Abe, Y. Hisaeda, *Angew. Chem. Int. Ed.* **2021**, *60*, 2614–2618; *Angew. Chem.* **2021**, *133*, 2646–2650; j) K. Nakao, H. Sasabe, Y. Shibuya, A. Matsunaga, H. Katagiri, J. Kido, *Angew. Chem. Int. Ed.* **2021**, *60*, 6036–6041; *Angew. Chem.* **2021**, *133*, 6101–6106; k) S. W. Kwak, H. Jin, J. H. Lee, H. Hwang, M. Kim, Y. Kim, Y. Chung, K. M. Lee, M. H. Park, *Inorg. Chem.* **2019**, *58*, 2454–2462.

[9] S. Katsuta, *Chem. Lett.* **1994**, *23*, 1239–1242.

[10] X.-F. Zhang, J. Zhu, *J. Lumin.* **2019**, *205*, 148–157.

[11] W. Wan, M. S. Silva, C. D. McMillen, S. E. Creager, R. C. Smith, *J. Am. Chem. Soc.* **2019**, *141*, 8703–8707.

[12] G. Li, D. Zhu, X. Wang, Z. Su, M. R. Bryce, *Chem. Soc. Rev.* **2020**, *49*, 765–838.

[13] a) S. D. Allen, D. R. Moore, E. B. Lobkovsky, G. W. Coates, *J. Organomet. Chem.* **2003**, *683*, 137–148; b) H.-C. Chiu, A. J. Pearce, P. L. Dunn, C. J. Cramer, I. A. Tonks, *Organometallics* **2016**, *35*, 2076–2085.

[14] Deposition number 2082119 (for **1**) contains the supplementary crystallographic data for this paper. These data are provided free of charge by the joint Cambridge Crystallographic Data Centre and Fachinformationszentrum Karlsruhe Access Structures service.

[15] a) S. Li, M. Wang, B. Liu, L. Li, J. Cheng, C. Wu, D. Liu, J. Liu, D. Cui, *Chem. Eur. J.* **2014**, *20*, 15493–15498; b) F. Yan, S. Li, L. Li, W. Zhang, D. Cui, M. Wang, Y. Dou, *Eur. J. Inorg. Chem.* **2019**, 2277–2283.

[16] a) J. Lewiński, I. Justyniak, J. Zachara, E. Tratkiewicz, *Organometallics* **2003**, *22*, 4151–4157; b) V. C. Gibson, D. Nienhuis, C. Redshaw, A. J. P. White, D. J. Williams, *Dalton Trans.* **2004**, 1761–1765; c) A. Arbaoui, C. Redshaw, D. L. Hughes, *Chem. Commun.* **2008**, 4717–4719; d) J. Liu, N. Iwasa, K. Nomura, *Dalton Trans.* **2008**, 3978–3988.

[17] a) F. Qian, K. Liu, H. Ma, *Dalton Trans.* **2010**, *39*, 8071–8083; b) A. Rösch, F. Seifert, V. Vass, H. Görls, R. Kretschmer, *New J. Chem.* **2021**, *45*, 972–981.

[18] a) A. Dreuw, J. Plötner, L. Lorenz, J. Wachtveitl, J. E. Djanhan, J. Brüning, T. Metz, M. Bolte, M. U. Schmidt, *Angew. Chem. Int. Ed.* **2005**, *44*, 7783–7786; *Angew. Chem.* **2005**, *117*, 7961–7964; b) S. H. Habenicht, S. Kupfer, J. Nowotny, S. Schramm, D. Weiß, R. Beckert, H. Görls, *Dyes Pigm.* **2018**, *149*, 644–651.

[19] F. Würthner, T. E. Kaiser, C. R. Saha-Möller, *Angew. Chem. Int. Ed.* **2011**, *50*, 3376–3410; *Angew. Chem.* **2011**, *123*, 3436–3473.

[20] G. A. Crosby, J. N. Demas, *J. Phys. Chem.* **1971**, *75*, 991–1024.

[21] a) *Principles of Fluorescence Spectroscopy* (Ed.: J. R. Lakowicz), Springer US, Boston, MA, **2006**; b) D. Zhai, W. Xu, L. Zhang, Y.-T. Chang, *Chem. Soc. Rev.* **2014**, *43*, 2402–2411; c) X. Ma, R. Sun, J. Cheng, J. Liu, F. Gou, H. Xiang, X. Zhou, *J. Chem. Educ.* **2016**, *93*, 345–350; d) Q. Li, Z. Li, *Adv. Sci.* **2017**, *4*, 1600484; e) J. Qi, X. Hu, X. Dong, Y. Lu, H. Lu, W. Zhao, W. Wu, *Adv. Drug Delivery Rev.* **2019**, *143*, 206–225.

[22] R. Datta, T. M. Heaster, J. T. Sharick, A. A. Gillette, M. C. Skala, *J. Biomed. Opt.* **2020**, *25*, 71203.

[23] a) A. Camposeo, L. Persano, D. Pisignano, *Macromol. Mater. Eng.* **2013**, *298*, 487–503; b) A. Camposeo, M. Moffa, L. Persano in *Electrospinning for High Performance Sensors* (Eds.: A. Macagnano, E. Zampetti, E. Kny), Springer International Publishing, Cham, **2015**; c) G. George, Z. Luo, *Curr. Nanosci.* **2020**, *16*, 321–362.

[24] a) H. Fong, I. Chun, D. H. Reneker, *Polymer* **1999**, *40*, 4585–4592; b) Y. Liu, J.-H. He, J.-y. Yu, H.-m. Zeng, *Polym. Int.* **2008**, *57*, 632–636.

Manuscript received: December 22, 2021
Accepted manuscript online: February 2, 2022
Version of record online: February 28, 2022